NUCLEAR DATA AND MEASUREMENTS SERIES

ANL/NDM-31

Titanium I: Fast Neutron Cross Section Measurements

by

P. Guenther, D. Havel, A. Smith, and J. Whalen

May 1977

NUCLEAR DATA AND MEASUREMENTS SERIES

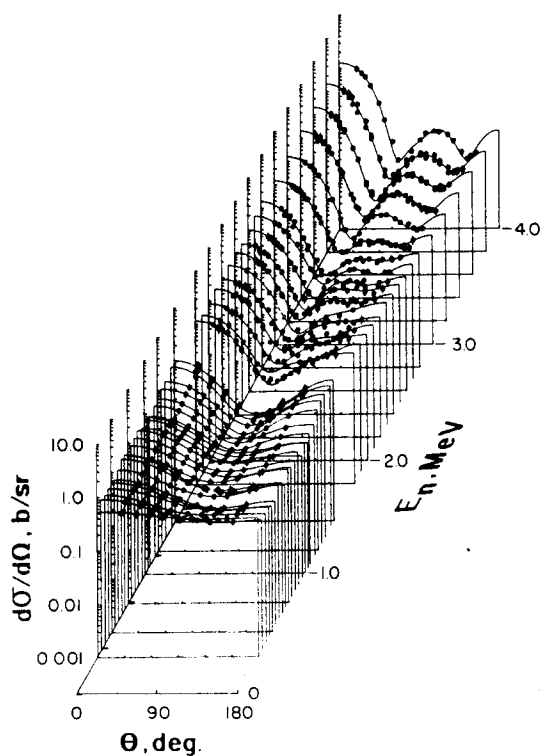ANL/NDM-31

TITANIUM-I; FAST NEUTRON CROSS SECTION MEASUREMENTS

by

P. Guenther, D. Havel, A. Smith and J. Whalen

May 1977

ARGONNE NATIONAL LABORATORY,
ARGONNE, ILLINOIS 60439, U.S.A.

ANL/NDM-31

TITANIUM-I; FAST NEUTRON CROSS SECTION MEASUREMENTS

by

P. Guenther, D. Havel, A. Smith and J. Whalen

May 1977

Applied Physics Division
Argonne National Laboratory
9700 South Cass Avenue
Argonne, Illinois 60439
U.S.A.

NUCLEAR DATA AND MEASUREMENTS SERIES

The Nuclear Data and Measurements Series presents results of studies in the field of microscopic nuclear data. The primary objective is the dissemination of information in the comprehensive form required for nuclear technology applications. This Series is devoted to: a) measured microscopic nuclear parameters, b) experimental techniques and facilities employed in measurements, c) the analysis, correlation and interpretation of nuclear data, and d) the evaluation of nuclear data. Contributions to this Series are reviewed to assure technical competence and, unless otherwise stated, the contents can be formally referenced. This Series does not supplant formal journal publication but it does provide the more extensive information required for technological applications (e.g., tabulated numerical data) in a timely manner.

TABLE OF CONTENTS

TITANIUM-I; FAST NEUTRON CROSS SECTION MEASUREMENTS[*]

by

P. Guenther, D. Havel, A. Smith and J. Whalen

Argonne National Laboratory
Argonne, Illinois   60439, U.S.A.

ABSTRACT

Energy averaged total neutron cross sections are measured from $\approx$ 1.0 to 4.5 MeV with few percent statistical accuracies. Differential elastic neutron scattering angular distributions are measured from 1.5 to 4.0 MeV at incident neutron energy intervals of $\leq$ 0.2 MeV. Differential cross sections for the inelastic neutron excitation of "states" at 158±26, 891±8, 984±15, 1428±39, 1541±30, 1670±80, 2007±8, 2304±22, 2424±16 and 2615±10 keV are measured for incident neutron energies from 1.5 to 4.0 MeV. Additional "states" are observed at approximately 2845 and 3009 keV. An energy-averaged optical-statistical model is deduced from the measured values and the implications of its use in the context of the strong fluctuating structure is discussed.

I. INTRODUCTION

The primary objective of this work was the provision of microscopic neutronic data for applied needs particularly at higher energies such as encountered in CTR conceptual energy systems (1) and in damage- and dosimetry-oriented applications including thermal reactors, fast reactors and CTR systems (2). This document (Titanium-I) is the first of two dealing with titanium and reports the results of neutron total and scattering cross-section measurements and the development of associated energy-averaged models suitable for subsequent extrapolation and evaluation. Extensive experimental studies of neutron induced reactions with titanium relevant to dosimetry applications have been previously reported (3). The companion report (Titanium-II) defines a complete evaluated nuclear data file in the ENDF format (4,5). In addition, a specific report of evaluated titanium dosimetry cross sections is given in Ref. 6.

II. EXPERIMENTAL METHODS

A. Samples

The measurement samples were fabricated from natural titanium metal having a chemical purity of greater than 99 percent. The scattering samples were right cylinders 2 cm in diameter and 2 cm long with neutrons incident on their lateral surfaces. The total cross-section measurement samples were 2.54 cm diameter cylinders with neutrons incident upon their bases. Three total-cross-section samples were used with lengths of 2, 3, and 6 cm. It was assumed that the samples were of uniform density and the measured atom-densities were very close to those given in conventional handbooks.

B. Total-Neutron-Cross-Section Measurements

The total neutron cross sections were deduced from the observed trans-
missions of approximately-monoenergetic neutron beams through the samples in
an axial direction (7). The cross sections were concurrently determined using
the three thicknesses of titanium samples and a carbon reference sample. The
incident neutron resolution was 125-135 keV as referenced to the threshold of
the $^7Li(p,n)^7Be$ reaction used as a neutron source. The energy scale was
determined to within ± 5 keV by control of the proton beam and verified by the
observation of well known resonance energies (e.g. the 2.078 MeV resonance of
carbon (8)). Experimental perturbations such as background, dead-time and
in-scattering effects were kept as small as practicable and appropriate
corrections were made. The "true" energy-averaged total neutron cross section
was determined by extrapolating the results obtained with the three titanium
samples of widely different thickness to a zero-thickness value. The details
of the experimental method, the data reduction procedures, and the total-cross-
section results have been extensively described elsewhere (9).

C. Differential-Neutron-Scattering Measurements

Elastic- and inelastic-neutron-scattering distributions were measured at
ten or more scattering angles using a 10-angle fast-neutron time-of-flight
system (10). The relative angular scale was optically determined to within
< 1 deg. and the absolute scale of the angular system was established to
within $\lesssim$ 1 deg. by the observation of the energy loss of neutrons scattered
from hydrogen at a number of angles both left and right of the incident-neutron
center line. The neutron source was the $^7Li(p,n)^7Be$ reaction pulsed for
durations of $\sim$ 1 nsec at a repetition rate of 2 MHz. The relative source
intensity was monitored using both collimated time-of-flight systems and long
counters. The scattered neutron flight paths were $\sim$ 5 m and defined by a

massive collimator system. The scattering samples were placed $\approx$ 13 cm from the source at a zero-degree reaction angle and at the common focus of the fli paths. Incident energy resolutions varied from 25 to 50 keV and the average energy scale was believed known to within ± 10 keV. The relative energy-dependent sensitivities of the ten detection systems were determined either b the observation of neutrons scattered from hydrogen (polyethylene) at a numbe of angles and a fixed incident energy or by the observation of the energy distribution of neutrons emitted from the spontaneous fission of ^{252}Cf (11). The absolute normalization of the relative detector sensitivities was determined by observation of neutrons scattered from hydrogen at each incident energy and at a selection of scattering angles (12). The calibration procedures were largely independent for each of the ten detectors. These methods resulted in scattering-cross-section results relative to the well known H(n,n) cross sections (13). Elastic neutron scattering cross sections of carbon were determined concurrently with those of titanium in order to validate the performance of the measurement system relative to the known angle-integrated elastic scattering cross sections of carbon (14). All titanium, carbon and hydrogen results were corrected for beam attenuation, angular resolution, and multiple event effects using a combination of analytical and Monte-Carlo procedures (15). The details of the experimental procedures and data treatment have been extensively discussed elsewhere (10, 11, 12 and 15).

III. EXPERIMENTAL RESULTS

A. Neutron Total Cross Sections

The total-cross-section measurements were made at energy intervals of $\lesssim$ 50 keV from $\approx$ 1.0 to 4.5 MeV. The emphasis was on accurate energy-average magnitudes comparable with the neutron scattering results (below) and suitable

for the development of energy-average models (e.g. optical model). The detailed definition of the resonance structure was specifically avoided. Cross sections were independently determined using the three sample thicknesses, 2, 3, and 6 cm. The statistical uncertainties of cross sections obtained with the 2 and 3 cm samples were 1-2 percent and those obtain with the 6 cm sample << 1 percent. The differences between cross section results obtained with the three sample thicknesses varied with energy, reflecting changes in the under-lying resonance structure. However, as expected, there was a systematic tendency for the cross sections obtained with the thinner samples to be larger than those obtained with the thicker sample. This trend decreased with increasing energy to negligible values in the 4.0 to 4.5 MeV range. Presumably, at higher energies the true resonance structure has considerably broadened and the cross section is tending more toward the smooth behavior that would not be sensitive to sample thickness. The results were corrected to zero-sample thickness by linearly extrapolating from the results obtained with the three different sample thicknesses. These zero-sample-thickness cross-section values are illustrated in Fig. 1. The statistical uncertainties were estimated to be $\sim$ 1 percent and this was supported by comparisons of concurrently measured carbon cross sections with precision values reported elsewhere (9,14).

The present broad-resolution results can be compared with average values derived from much better resolution measurements such as those of Ref. 14. The results of Ref. 14 were averaged using a square resolution function with widths of 100 and 150 keV centered on the mean energy of each of the present measurements. There were uncertainties in this averaging procedure due to a lack of knowledge of the detailed nature of the respective resolution functions. However, the two averages cover the range of experimental resolutions employed in the present measurements and their general behavior was not very different

as illustrated in Fig. 1. The average values derived from the better resolution measurements are 5 to 10 percent lower than the present broad resolution results at energies of < 3.0 MeV. This difference decreases to 2 to 4 percent at 4.0 MeV. At the lower energies the difference is well beyond the statistic uncertainties of the respective measurements. The difference could not be explained as an error in the present measurements and the concurrent determinations of carbon cross sections agreed with those reported by Schwartz et al. (14) to within $\approx$ 1 percent. The titanium measurements of Ref. 14 employed relatively thick samples (10.7 cm) that, with the broad resolutions of the present experiments, would lead to cross section values 5 to 10 percent too low; i.e. very near the discrepancy between the present results and the average of those of Ref. 14. The sample-size effect is mitigated by improved resolution and the multi-isotopic nature of elemental titanium but theoretical estimates indicate that the resonance extrema in the low MeV range may be much larger than experimentally observed with the best resolution measurements (16). It is possible that the thick samples of Ref. 14 resulted in a very "dark gray" response at the true resonance maximums with a consequent under-determination of the average total cross section magnitudes even with relative good resolution.

More details of the above total cross section measurements and some suggested implications of the broad resolution interpretations of fluctuating-resonance structure are discussed in Ref. 9.

B. Neutron Elastic Scattering Cross Sections

The differential elastic neutron scattering cross sections were measured at incident-neutron energy intervals of $\lesssim$ 200 keV from 1.5 to 4.0 MeV with resolutions of 25 to 50 keV. The measurements at each incident energy were made at ten or more scattering angles distributed between $\approx$ 20 and 160 deg.

The estimated uncertainties were: < 1 to 5 percent due to counting statistics, 3 to 5 percent due to normalization procedures, and 2 to 5 percent due to correction procedures. Thus the overall RMS uncertainties were in the range 5 to 10 percent. The experimental results and their respective uncertainties are outlined in Fig. 2. It is evident that these angular distributions fluctuate with energy as would be expected from the total cross sections of Fig. 1. These fluctuations are enhanced in the single elastic channel and by a finer experimental energy resolution than used in obtaining the total cross section results. Small variations in incident resolution or energy scale can change the observed distributions by large amounts. For these reasons measurements made at different times were not always consistent. However, some of the distributions of Fig. 2 are composites of two or more data sets obtained at widely different times, (e.g. the 3.0 MeV distribution) and the results are in good agreement.

The measured distributions were least-square fitted with Legendre polynomial expansions in order to determine the angle-integrated elastic neutron scattering cross sections shown in Fig. 1. The fitting procedures were unconstrained thus the distributions calculated from the fits may not be representative of true values beyond the measured angular range. The deduced angle-integrated elastic scattering cross sections were believed known to ~ 5 percent. Contributing to this uncertainty was a sample-size effect of the same nature as outlined above in the context of the total neutron cross sections. The scattering samples were small but, even so, the scattering results may be systematically biased toward too low values by several percent. Appropriate corrections are difficult as there is no high-resolution experimental information and reliance must be placed upon theoretical estimates of structure. Experimental determinations of the correction factors would be tedious and

subject to increasing statistical uncertainties as the sample size decreased. In the present work it was assumed that the samples were small enough to make the size effects a relatively minor contribution to the overall uncertainties. The present angle-integrated elastic scattering results were consistent within the respective uncertainties and varying resolutions with the present neutron total and inelastic scattering results (outlined below). This is less true of the averages of the total cross sections of Ref. 14 as the latter tend to closely approach the elastic scattering cross sections at some energies where the non-elastic scattering cross section is known to be appreciable.

The present 1.5 MeV-data are very similar in relative-angular-dependent shape to a 1.4 to 1.5 MeV average of the values of Ref. 16. There is a normalization difference that is well within what one might expect from the different energies and resolutions in the context of the inherent fluctuations. The present 3.2 MeV results are not in particular agreement with the comparable distribution of Ref. 17 but the present results reasonably extrapolate to the 4.1 MeV results of Walt et al. (18) excepting the very largest-angle values. It is not clear how significant any of these agreements or disagreements are in view of the fluctuations and experimental variations in both energies and energy resolutions. More quantitative comparisons require averages over a data basis of larger energy scope than available in the literature. Comparisons of single distributions in the present context are unrewarding and even deceptive.

C. Neutron Inelastic Scattering Cross Sections

Inelastically scattered neutrons were quantitatively observed corresponding to the excitation of states in titanium at energies of $\lesssim$ 3.0 MeV. The excitation of higher-energy states was observed in a more qualitative and less reliable manner. The excitation energies were determined from the measured

scattered-neutron flight times and the known incident neutron energies and were verified by the observation of neutron groups resulting from the excitation of well known states in other nuclei (e.g. the 846 keV state of ^{56}Fe). The mean energies of the observed states were determined from a simple average of the measured values, in one case more than 50 independent determinations. The corresponding uncertainties were generally defined as RMS deviations of the observations from the mean. In all, 12 states were observed with energies of: 158±26, 891±8, 984±15, 1428±39, 1541±30, 1670±80, 2007±8, 2304±22, 2424± 16, 2615±10, 2845±(?) and 3009±(?) keV; the latter two are less reliable. The uncertainties reflect contributions from measurement techniques, the relative intensities involved, and the complexity of the underlying structure contributing to the observation. The latter factor was significant as illustrated by the relatively large uncertainty associated with the 1670-keV "state" which was undoubtedly made up of a number of components from the odd titanium isotopes.

The above experimental results are compared with structures reported in the literature in Table 1 (19). The first, second and third observed states are clearly associated with levels in ^{47}Ti, ^{46}Ti, and ^{48}Ti, respectively. The observed excitations at energies of $\gtrsim$ 1.0 MeV all appear to contain contributions from two or more isotopes. Of course, the observations were dominated by contributions from the by far most abundant isotope, ^{48}Ti(74%). The present results are generally consistent with previously reported structures with the exception of the 1247- and 1793+1821-keV states in ^{47}Ti. Contributions due to the former were not observed probably due to the relatively low intensity and small isotopic abundance. The same factors effect the observation of the 1793+1821-keV doublet and, in addition, its small contribution may have been incorporated within the broad group observed at 1670 keV.

Generally, an intent of the present energy determinations was a correlation of the measured values with known structure in the titanium isotopes which has been more precisely determined using other methods.

Angle-integrated cross sections for the excitation of observed "states", outlined in Table 1, were determined by least-square fitting a Legendre polynomial series to the measured angular distributions. A minimum of four differential values were required for this fitting procedure and more than fifty were available in some instances. Most of the observed inelastically scattered neutron distributions approached isotropy as illustrated in Fig. 5. The uncertainties associated with the individual angle-integrated values varied widely from a minimum value of $\sim$ 5 percent, relevant to prominent and well defined cross sections, to $\sim$ 50 percent for very small and poorly defined cross sections. The factors influencing elastic scattering uncertainties (above) were applicable and, in addition, some of the inelastic scattering results were far more sensitive to uncertainties associated with background and resolution effects. The present angle-integrated inelastic scattering results are summarized in Fig. 3 and compared with experimental values obtained elsewhere and with the evaluation of Ref. 4 (i.e. Titanium-II).

The first observed state at 158 keV is attributed to the minor odd isotope ^{47}Ti($\frac{7}{2}$ -). The corresponding cross sections are small and difficult to observe, therefore, the uncertainties are relatively large.

The 891-keV state is also due to a minor isotope, ^{46}Ti(2+), and the scattered neutrons are difficult to resolve from those due to the neighboring prominent 984-keV state. The present cross sections are small and relatively uncertain but consistent with the lower energy values of Ref. 16.

The excitation of the 984-keV state, ^{48}Ti(2+), is the prominent feature of inelastic neutron scattering in the energy range of the present measure-

ments. The cross sections are large and fluctuate with energy. The present results are generally consistent within experimental uncertainties of as little as $\sim$ 5 percent despite these fluctuations and the random scheduling of the measurements over a several-year period. The present results are consistent with those of Holmqvist et al. (20) and reasonably extrapolate to the lower energy results of Ref. 16. The agreement with some other previous results reported from direct-neutron and (n;n',γ) measurements is not as good (21-25). However, many of these differences are within a range reasonably attributable to fluctuations and varying resolutions. Moreover, (n;n',γ) results are not unambiguously related to neutron scattering cross sections in all cases.

The observed excitations of higher lying states (No. 4-12 of Table 1) are unquestionably due to a complexity of unresolved contributions from a number of the titanium isotopes. The cross sections are generally small as illustrated in Fig. 3. Comparable experimental results are largely confined to the work of Holmqvist et al. (20). The latter generally agree with the present results when the two sets of values are combined so as to reflect comparable experimental resolutions. Neither set of measurements has enough resolution to fully resolve the isotopic components as outlined in Table 1 thus comparisons are realistic only over rather broad excitation "bands" as illustrated in Fig. 3.

IV. CALCULATIONAL MODELS

The calculational objective was an energy-average model suitable for the interpolation and extrapolation of measurements in the subsequent titanium evaluations (4). It was not the intent to develop a generalized model though the results may have a wider applicability. The model was based upon the

isotope ^{48}Ti. The excited structure of this isotope is known to 4 MeV thus the various reaction-channel contributions can be calculated at the energies of the present experiments (19). Approximately, seventy-five percent of the element consists of this isotope and another eight percent is due to the structurally-similar isotope ^{46}Ti. The remaining constituents are approximately equally distributed between the three odd isotopes of titanium. The latter contributions should not have a significant impact on the model and its intent.

The derivation of the model was based upon a 6-parameter χ1-square fit of a spherical optical potential to each of the 18 elastic scattering distributions measured at incident energies of 1.5 to 4.0 MeV. Compound-elastic-scattering contributions were calculated using the Hauser-Feshbach formalism with width fluctuation corrections (26,27). The resulting potential parameters varied from distribution to distribution reflecting the evident energy dependent fluctuations. Generally, the parameter sets fell into two classes. Class-I was characterized by relatively deep real potentials ($\approx$ 50 MeV) and narrow radii and was representative of 80 to 90 percent of the results. Class II was characterized by larger radii and smaller real potential strengths ($\approx$ 45 MeV) and was applicable at lower incident energies. This ambiguity in potentials has been noticed on previous occasions and is reflected in the literature (28,29). In some cases repeated fits to a given distribution resulted in convergence to either class. The general potential derived from the present measurements was obtained by averaging the parameters obtained from the fits of the Class-I type to the individual distributions. The respective parameter uncertainties were defined as the RMS deviation from the mean. This uncertainty definition combines effects due to statistical uncertainties of the data and to physical fluctuations from distribution to distribution.

The latter are the dominant factor and, therefore, the parameter uncertainties tend to reflect the variance in potentials in this mass-energy region due to inherent physical fluctuations.

The above methods and the present experimental values provide little guidance as to the energy dependence of the potential. The latter was examined in the context of total neutron cross sections over the energy range 0.2 to 20.0 MeV. Total neutron cross sections calculated with the above potential were fairly consistent with the measured values (as summarized by the evaluation of Ref. 4) with no energy dependence of the potential as illustrated in Fig. 4. A positive energy dependence of the real potential gave an improved agreement with measured values but was rejected as being physically questionable. At lower energies the resonance structure makes comparisons with the model subjective but the general trends of the total-cross-section minimum in the region 0.6 to 2.0 MeV are reasonably represented. At higher energies the calculations are similar to the measured values with the largest discrepancies of 4 to 6 percent in the 4 to 6 MeV region. The latter difference may, in part, be partly due to experimental uncertainties. In the energy range of the present total-cross-section measurements, the calculated values were a few percent lower than the measured total-cross sections, as illustrated in Fig. 1, in some energy regions. This difference may be associated with fluctuations of the measured values. Few-percent sample-thickness perturbations in the elastic scattering measurements (noted above) could also be a factor. The calculated ℓ_0 strength function is 3.3 x 10^{-4} which is consistent with the value 4.9 ($\pm$ 2.2) x 10^{-4} reported from low energy resonance measurements (30).

The above model was re-examined in the context of a simple one phonon dynamic vibrator coupling the ground (0+) and first excited (2+) states (31). This additional complexity did not particularly improve the description of the

present experiments or of the broader-scope-total neutron cross sections. Therefore, the coupled-channel calculations were limited to considerations of direct excitations of the first (2+) state. The direct-excitation component was not large relative to the compound-nucleus component and the calculated anisotropies of the scattered neutrons relatively small. Such small anisotropies with a forward-angle bias were marginally evident in some of the measured distributions as illustrated by the 3.6 MeV results for the 984 keV state shown in Fig. 5. Quantitative calculation of such distributions was thwarted by uncertainties in the interpretation of the primary compound-nucleus component.

The numerical parameters of the present potential are summarized in Table 2. This potential is very similar to the general form proposed by Holmqvist and Weidling (29). Several other potentials reported in the literature were examined in the context of total neutron cross sections; for example, the generalized potential of Becchetti and Greenlees (32), the neutron potential of Wilmore and Hodgson (33), the proton-based potential of Perey (34), and the neutron potential of Engelbrecht and Fiedeldey (28). The latter belongs to the above Class-II and generally gave the best descriptions of the total cross sections over a broad energy range. This latter potential has a volume absorption the effects of which were minor in the energy region of present interest. Some of the other potentials gave a better description of the total cross section in the 4 to 6 MeV region than obtained with the present model but were less suitable at higher or lower energies or both. The general trend in these cases was toward too large cross sections in the region 0.6 to 2.0 MeV.

In view of the above, the potential of Table 2 appeared reasonably suitable and was accepted for subsequent applications. It gives a reasonable

description of the total-neutron cross sections (Figs. 1 and 4) and of the average trend of differential elastic and inelastic neutron scattering cross sections. It will not necessarily quantitatively describe any particular measured elastic-scattering distribution. This is illustrated by the 3.0 and 3.6 MeV comparisons of Fig. 5. The calculated results are reasonably descriptive of the 3.0 MeV measurements but less so at 3.6 MeV. Fluctuations make the latter distribution rather anomalous as evident from Fig. 2 and angle-integrated elastic scattering cross sections deduced from measurements at both energies tend to be larger than the average trend as illustrated in Fig. 1. Fig. 5 also illustrates the consequence of omitting the width fluctuation corrections to the Hauser-Feshbach formula. With the given potential of Table 2, the calculated uncorrected elastic distributions are very different from the corrected result and the measured values.

Inelastic neutron scattering cross sections were calculated only for those values attributable to ^{48}Ti (e.g. 984, 2304 and 2424 keV states). The calculated results are compared with the measured values in Figs. 3 and 5. All the calculated results are strongly dependent upon the fluctuation correction with the "corrected" result being pronouncedly lower than that calculated with the Hauser-Feshbach formula alone. Over much of the present experimental range the measured cross sections for the excitation of the prominent 984 keV state lie between the two calculated results. This suggests that fluctuation enhancement of the compound cross sections may be a factor in these processes as discussed by Moldauer (35). The exact nature of such an enhancement was not clear and the practical tools for implementing such a calculation were not available. Thus, in cases such as this, fluctuations in both experimental and calculational contexts make quantitative physical interpretation of both elastic and inelastic neutron scattering processes difficult and uncertain.

This is recognized in both the present intepetations and the subsequent applications of the model. In comparison, the possible contributions from collective vibrations (noted above) are relatively small at the energies of the present experiments and not an important consideration in the interpretat: of the present experiments.

V. SUMMARY REMARKS

These measurements provide a quantitative and internally consistent data base for the evaluation of elemental titanium neutron cross sections from $\sim$ 1.0 to 5.0 MeV. This data base includes both total cross sections and specific scattering channels that account for the very large majority neutron interactions with titanium in this energy range. The measured values provide accurate energy-average normalization points for the adjustment of higher resolution results (e.g. total neutron cross sections) and directly provide for applied cross section needs (e.g. neutron scattering cross sections). A model deduced from the measurements is useful for interpolation and extrapolation of measured values in the evaluation process. However, fluctuations, in both experimental and theoretical contexts, limit the quantitative applicability of the model until such time as improved physical understanding and associated calculational tools are available. A comprehensive evaluation utilizing these measurements and this model is discussed in the companion document, Titanium-II (4). That evaluation is submitted as an elemental contribution to the general ENDF/B-V evaluated-nuclear-data-file system. ·

ACKNOWLEDGMENTS

REFERENCES

1. Oak Ridge Natl. Lab. Report USNDC-CTR-1, (1974), Ed. D. Steiner, unpublished.

2. ENDF/B-IV Dosimetry File, Brookhaven Natl. Lab. Report BNL-NCS-50446 (1975), Ed. B. Magurno.

3. D. Smith and J. Meadows, Cross Sections for (n,p) Reactions on ^{27}Al, ^{46,47,48}Ti, ^{54,56}Fe, ^{58}Ni, ^{59}Co, and ^{64}Zn from Near Threshold to 10 MeV, Argonne Nat. Lab. Report ANL/NDM-10 (1975).

4. C. Philis et al., Argonne Natl. Lab. Report, to be published. Herein referred to as "Titanium II".

5. Brookhaven Natl. Lab. Report BNL-NCS-50496 (1975), Eds. D. Garber et al.

6. C. Philis, O. Besillon, D. Smith, and A. Smith, Evaluated (n;p) Cross Sections of ^{46}Ti, ^{47}Ti and ^{48}Ti, Argonne Natl. Lab. Report ANL/NDM-27 (1977).

7. D. Miller, Fast Neutron Physics, Part 2, Eds. J. Marion and J. Fowler, Interscience Pub. N.Y. (1963).

8. J. Meadows, Argonne Natl. Lab. Report ANL/NDM-25 (1977).

9. A. Smith and J. Whalen, Comments on the Energy-Averaged Total Neutron Cross Sections of Structural Materials in the Few MeV Range, Argonne Nat. Lab. Report ANL/NDM-28 (1977).

10. A. Smith, P. Guenther, R. Larsen, C. Nelson, P. Walker and J. Whalen, Nucl. Inst. and Methods, 50 277 (1967).

11. A. Smith, P. Guenther and R. Sjoblom, Nucl. Inst. and Methods, 140 397 (1977).

12. P. Guenther, A. Smith and J. Whalen, Phys. Rev., C12 1797 (1975).

13. J. Hopkins and G. Breit, Nucl. Data, A9 137 (1971).

14. R. Schwartz, R. Schrack and H. Heaton, MeV Total Neutron Cross Sections,

Natl. Bur. of Stds. Pub. NBS-138 (1974).

15. P. Guenther, Univ. of Ill. Thesis (1977).

16. E. Barnard, J. deVilliers, P. Moldauer, D. Reitmann, A. Smith and

    J. Whalen, Neutron Scattering from Titanium; Compound and Direct Effects,

    Argonne Natl. Lab. Report ANL/NDM-3 (1973).

17. R. Becker, W. Guindon and G. Smith, Nucl. Phys., 89 154 (1966).

18. M. Walt and J. Beyster, Phys. Rev., 98 677 (1955).

19. Nuclear Data Sheets for A=48, J. Rapaport (1970), See also Nuclear Data

    Sheets for minor isotopes.

20. B. Holmqvist et al., Aktiebolaget Atomenergi Report, AE-481 (1973).

21. K. Tsukada S. Tanaka and M. Maruyama, Jour. Phys. Japan, 16 166 (1961).

22. L. Cranberg and J. Levin, Phys. Rev., 103 343 (1956).

23. Broders et al., Fiz. Energ. Inst., Obniwsk Report, 32 (1965).

24. E. Konobeevski et al., Izv. Akad. Nauk SSSR, 37 1764 (1973).

25. Pasechnik et al., Ukrain. Fiz. Zhurnal, 14 1874 (1969).

26. W. Hauser and H. Feshbach, Phys. Rev., 87 366 (1952).

27. P. Moldauer, Phys. Rev., 135 B642 (1964).

28. C. Engelbrecht and H. Fiedeldey, Ann. Phys., 42, 262 (1967).

29. B. Holmqvist and T. Wiedling, Optical Model Analysis of Fast Neutron

    Elastic Scattering Data, Aktiebolaget Atomenergi Report, AE-430 (1971).

30. Brookhaven Natl. Lab. Report, BNL-325, 3rd Ed. Vol-1, Eds. S. Mughabghab

    and D. Garber (1973).

31. T. Tamura, Oak Ridge Natl. Lab. Report, ORNL-4152 (1967).

32. F. Becchetti and G. Greenlees, Phys. Rev., 182 1190 (1969).

33. D. Wilmore and P. Hodgson, Nucl. Phys., 55 673 (1964).

34. F. Perey, Phys. Rev., 131 745 (1963).

35. P. Moldauer, Proc. of the Inter. Conf. on the Interaction of Neutrons

With Nuclei, CONF-760715-P1 (1976).

36. W. Kinney and F. Perey, Oak Ridge Natl. Lab. Report, ORNL-4810 (1973).

Table 1. Excitation Energies as Observed in Inelastic Neutron Scattering Measurements

No.	E_x Observed[b] (in keV)	Attributed to E_x of Ref. 19 (in keV)
1	158 ± 26	159, 7/2-, Ti-47
2	891 ± 8	889, 2+, Ti-46
3	984 ± 15	983, 2+, Ti-48
4	1428 ± 39	1442, 11/2-, Ti-47 1382, 3/2-, Ti-49
5	1541 ± 30	1549, 3/2-, Ti-47 1542, 5/2-9/2-, Ti-49 1585, 3/2-, Ti-49 1554, 2+, Ti-50
6	1670 ± 80	1670, ?, Ti-47 1622, 5/2-9/2-, Ti-49 1723, ?, Ti-49 1762, 1/2-, Ti-49
7	2007 ± 8	2009, 4+, Ti-48
8	2304 ± 22	2295, 4+, Ti-48 Ti-47 (?) Ti-49 (?)
9	2424 ± 16	2421, 2+, Ti-48 Ti-47 (?) Ti-49 (?)
10	2615 ± 10	2611, 0+, Ti-46 Ti-47 (?) Ti-49 (?) 2677, 4+, Ti-50 (?)
11	2845[a] (?)	Ti-47 (?) Ti-49 (?)
12	3010[a] ± (?)	3000, 0+, Ti-48 Ti-47 (?) Ti-49 (?)

a. Insufficient values were available for a reliable determination of RMS uncertainties; i.e. ≤ 3.

b. Present experiments.

Table 2. Spherical Optical Model Parameters for Titanium

Real Potential

$$V^a = 50.01 \ (\pm \ 1.0)^b \ \text{MeV}$$

$$R_V^c = 1.221 \ (\pm \ 0.025), \ \text{F}$$

$$A_V = 0.533 \ (\pm \ 0.050), \ \text{F}$$

Imaginary Potential

$$W^d = 8.616 \ (\pm \ 1.2), \ \text{MeV}$$

$$R_W = 1.183 \ (\pm \ 0.08), \ \text{F}$$

$$A_W = 0.544 \ (\pm \ 0.1), \ \text{F}$$

---

a. Saxon-woods real form; Spin-orbin term of Thomas form (8 MeV).

b. All uncertainties RMS values derived from 16 distributions.

c. All radii expressed in form $R = R \cdot A^{1/3}$.

d. Derivative form.

FIGURE CAPTIONS

Fig. 1.   Measured neutron total (O) and elastic (□) scattering cross sections of elemental titanium. Present measured values are indicated by data points. Equivalent average cross sections constructed from Ref. 14 are indicated by ———————— (150 keV ave.) and — — — — — — — (100 keV ave.). The solid curves indicate the results of model calculations.

(ANL Neg. No. 116-77-336)

Fig. 2.   Measured differential elastic scattering cross sections of elemental titanium. Data points indicate the present measured values, curves the results of unconstrained Legendre polynomial fits to the measured values.

(ANL Neg. No. 116-77-335)

Fig. 3.   Inelastic neutron scattering excitation cross sections of elemental titanium. The present measured values are indicated by (O) data points. Other measured values are noted as follows: ✛ = Ref. 16, △ = Ref. 24, ◇ = Ref. 36, $\overline{X}$ = Ref. 23, Z = Ref. 20, Y = Ref. 21, and ⋈ = Ref. 22. The solid curves denote the evaluation of Ref. 4. Calculated results are given by: — — — Hauser-Feshbach result, and ······ Hauser-Feshbach with width fluctuation correction.

(ANL Neg. No. 116-77-398)

Fig. 4.   Comparison of calculated and evaluated total neutron cross sections of elemental titanium. The heavy curve indicates results calculated with the model of the text, the light curve the evaluation of Ref. 4.

(ANL Neg. No. 116-77-376)

Fig. 5.   Illustrative angular distributions of elastic and inelastic scattered neutrons. Present measured values are indicated by data points.

Incident energy and excitation energy are noted by E_{in}/E_x in MeV.
Curves indicate the results of model calculations where H = the
Hauser-Feshbach result and W = the Hauser-Feshbach result with
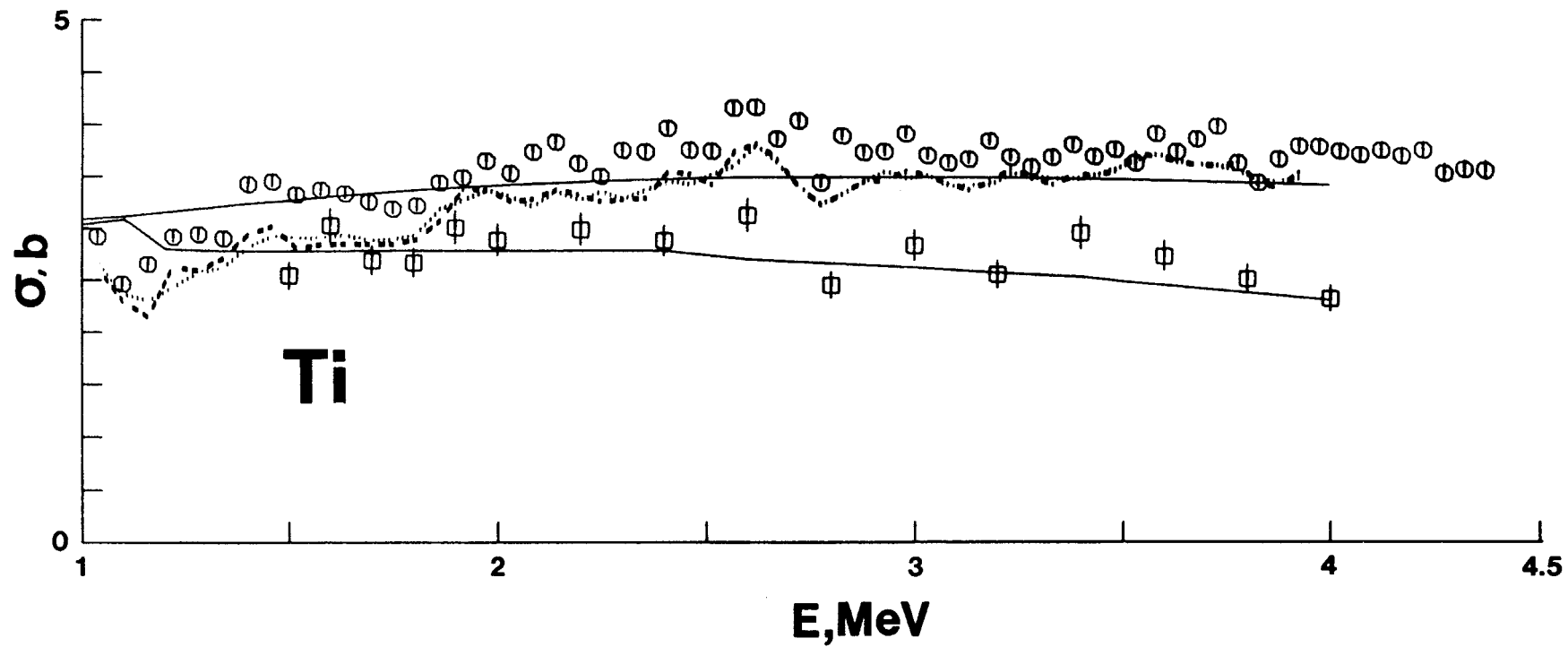width fluctuation correction.

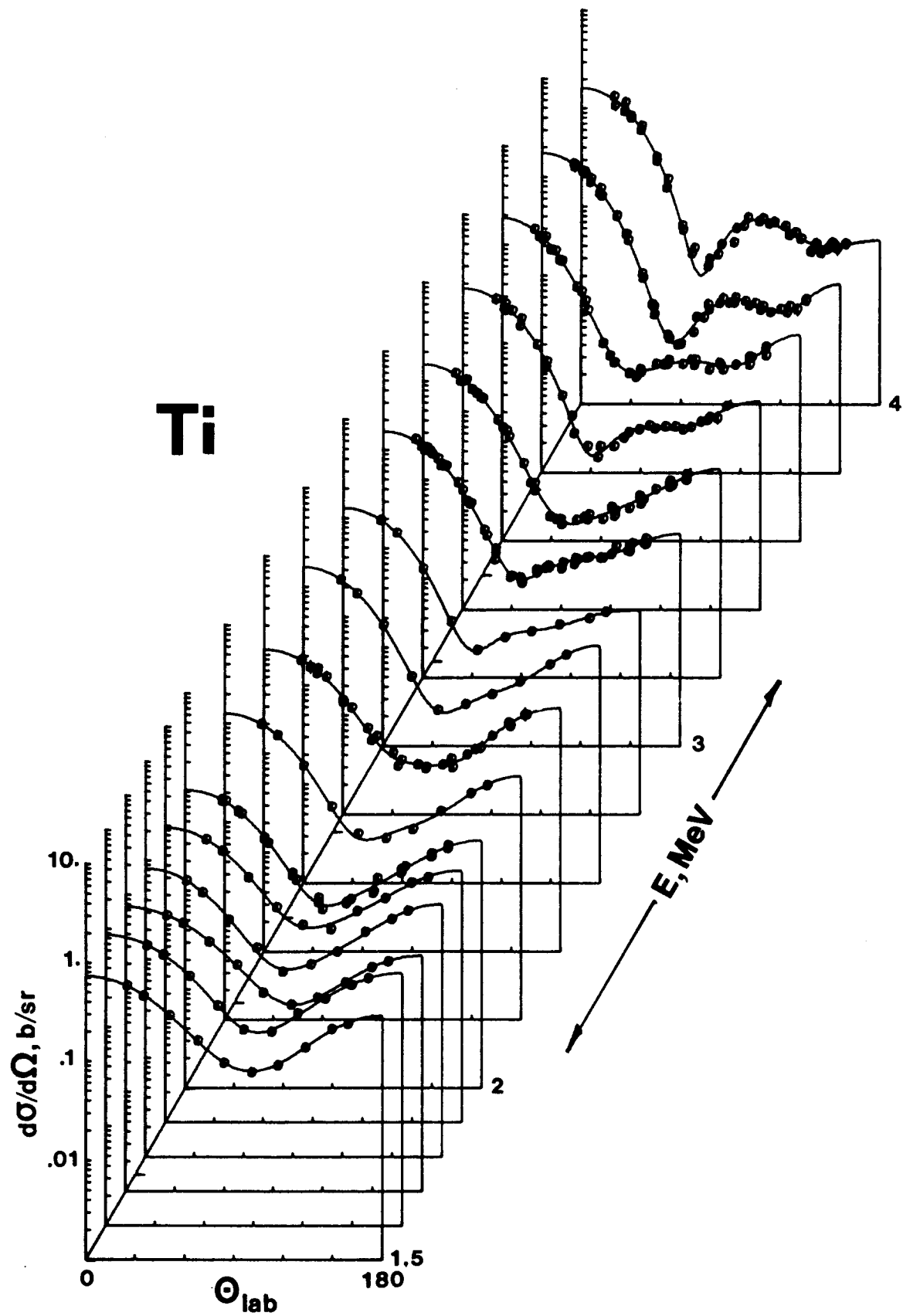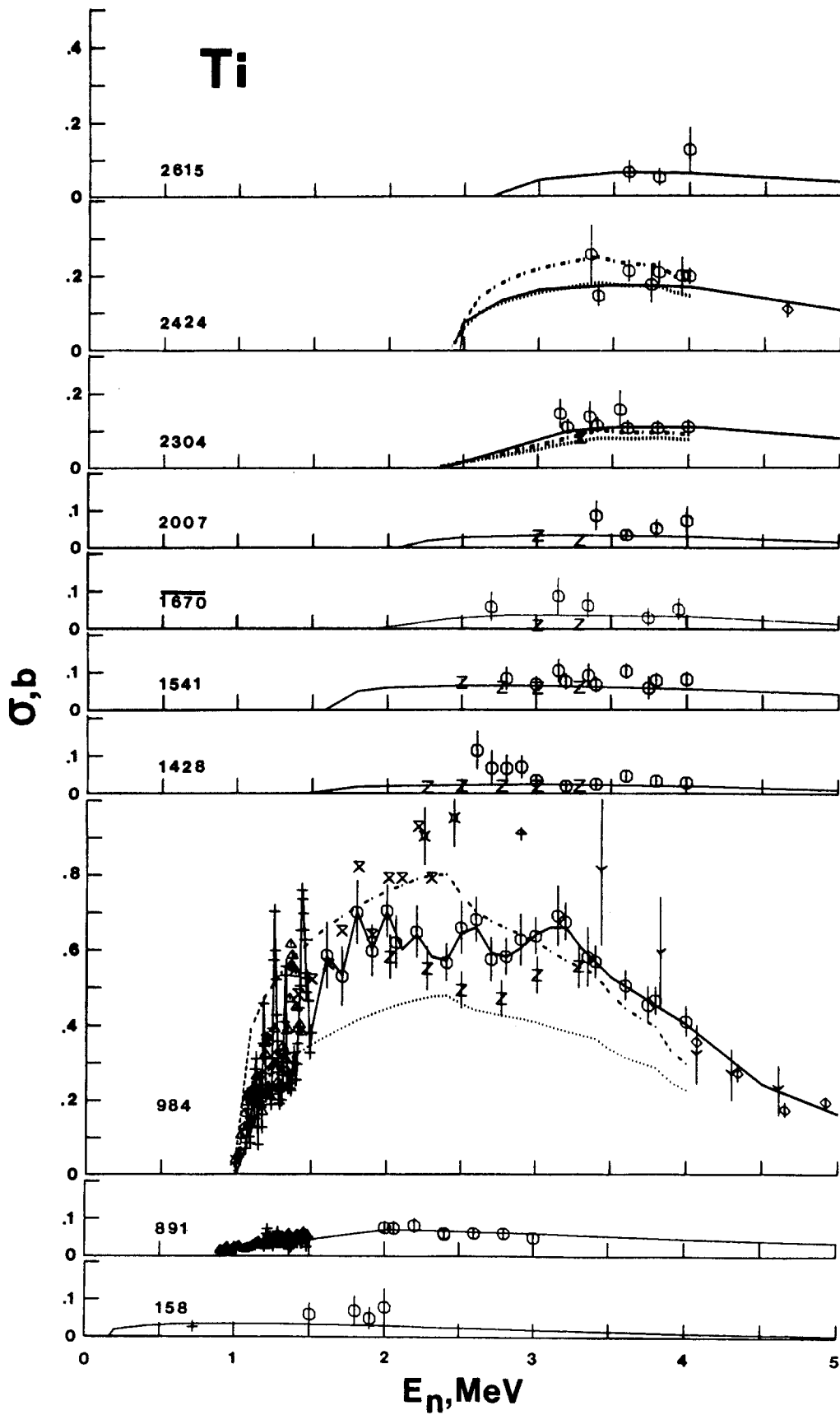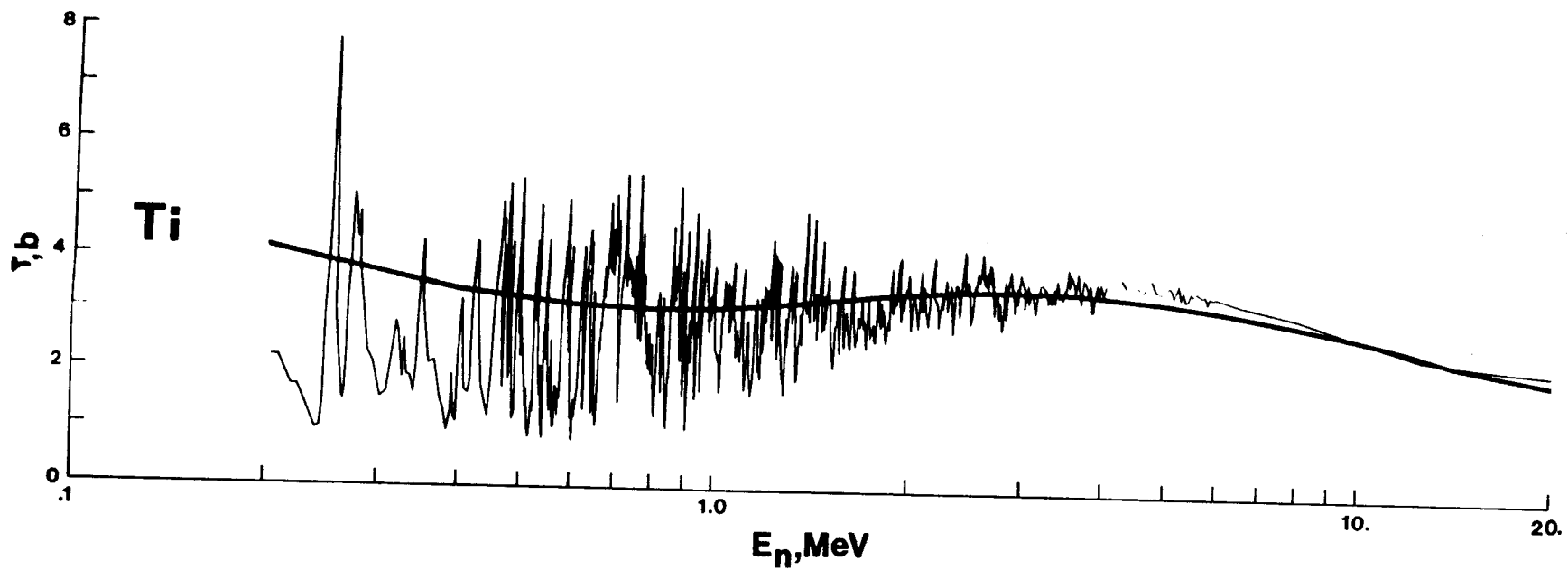(ANL Neg. No. 116-77-377)

Fig. 1

Fig. 2

Ti

d𝜎/dΩ, b/sr

10.

1.

.1

.01

0

Θ_lab

180

1.5

2

3

4

E, MeV

Fig. 3

Fig. 4

Fig. 5